Proceedings of the 4th International Conference on Recent Innovation in Engineering
ICRIE 2023, University of Duhok, College of Engineering, 13th – 14th September 2023
(Special issue for Passer journal of basic and applied sciences)
Paper No. 27

Review of using ceramic coatings to increase the performance of solar collectors with air brush spray method on stainless steel substrate

Saja Faleh Abdul Hadi[1,a)], Elham Abd Al-Majeed[1,b)], Hayder k. Rashid[1,c)]

[1]College of Material Engineering, Ceramic Engineering Department, University of Babylon, Babylon, Iraq.
Corresponding author: **Saja Faleh Abdul Hadi**
Email: saja.falh.math95@student.uobabylon.edu.iq

ABSTRACT:

In recent decades, our world is exposed to many of economic crisis comes from high energy prices due to steadily increasing demand for it. However, the most important source of energy that widely consumed is extracted from fossil fuels. Moreover, these energy production processes making planet to be exposed to in terms of environmental pollution. Where, because of the emission of carbon dioxide and other gases, which lead to global warming and high air temperatures, this is considered a threat to the environment. On the other hand, the renewable and sustainable energies are available all over the world, which is clean, non-polluting. Consequently, the mineral types of materials suitable for coating process were studied to improve the use of solar energy in pure water production processes. However, the coating process presented to improve the insulation of type 316 stainless steel basin. Where, the glass cover of the solar water desalination system is clear to allow sunlight to pass through it. So, the heat conductive component and the insulating basin maintain a suitable water temperature to make still water to be evaporated and then condensation at the glass surface then collecting pure water. Since, ceramic materials have better thermal insulation than other insulating coating materials; their application concern for enhancing insulation. In this work, the materials that used for improving the insulation of steel absorber plat are mullite, titanium oxide and magnesium oxide, polymer components are added to the paint mixture without changing the properties of the coating in order to increase the uniformity and adhesion of the materials used. X-ray diffraction (XRD), scanning electron microscopy (SEM) and (EDS), atomic force microscopy (AFM), spectrophotometer-infrared (FTIR), thermal conductivity, adhesion strength, hardness, density, porosity, viscosity test Coating thickness, ultraviolet (UV), wettability, and abrasion. For investigate the feature of coating metals, some of the tests that are performed for their effectiveness.

KEYWORDS: Desalination basin, stainless steel 316, spray airbrush, thermal insulation, mullite, titanium oxide, magnesium oxide and polymer.

1 INTRODUCTION

Renewable energy sources, such as solar and wind power, are readily available, inexpensive, and do not spoil the environment. Because of the cleanest, most affordable, and readily available energy sources, renewable energies have experienced remarkable growth all around the world. Numerous industries, including heating, chemical processing, and mechanical uses, have utilized solar energy[1]. However, the heat transfer is due to the conduction, convection and radiation processes with the environment; also depends on the local sun radiation conditions and the solar collector optical features[2]. as shown in figure (1).

T**he substrate** because of its extensive range of customizable qualities and all-around resilience to extreme environmental conditions, the stainless steel family stands out among all components of engineering [3].The austenitic stainless steel AISI 316L in particular is a technologically significant material that has been extensively employed in many different industrial sectors because of its superior resistance to corrosion in various engineering contexts [4]. Owing to its outstanding resistance to corrosion and biocompatibility, additionally, it has discovered to be applicable to biomedicine field for the creation of medical equipment and body implants[5].But in actual applications, it frequently experiences severe tribological concerns including excessive wear, scoring, and friction [6] because of relative weakness and softness. There have been attempts attempted to modify stainless steels' surfaces using a variety of processes, including Ceramic coating nitriding, carburising, and PVD deposition. The need for additional acceptable alternatives [7] is caused by the significant drop in Metal dusting brought on by carburising, corrosion resistance brought on by nitriding [6,] and inadequate coating adherence.

ceramic coating materials boost thermal insulation and lower emissivity, reducing heat loss and increasing collector performance efficiency. Selective coatings considered from cheaper and easier methods to improve collector efficiency[1] The use of insulating materials that contain large proportions of gaps and pores leads to a very large increase in insulation, as is the use of porous Mullite, the thermal conductivity value reaches to (0.09 w/m.k)[8]. The best selective coating ceramic materials that used to increase thermal insulation are (Al_2O_3, $3Al_2O_3.2SiO_2$, SiO_2, ZrO_2, YSZ, TiO_2, CeO_2, $La_2Zr_2O_7$ ...etc.)[9].

coating process Alternative coating techniques include electro-deposition coating, electrophoretic Physical vapor deposition (PVD), chemical vapor deposition (CVD), and electroplating (EPD) [10], and plasma spray coating, among others [11],thermal mist, high-velocity oxy-fuel coating, and sol-gel (HVOF). using a warm spray gun to apply coatings such as detonation, arc wire, and flame coating techniques including cold spraying, airbrushing, and coating[12].

The aim study of this research is to obtain thermal insulation through the use of ceramic materials that increase the insulation of stainless steel by coating it with one of the common methods, which is the air brush spraying method.

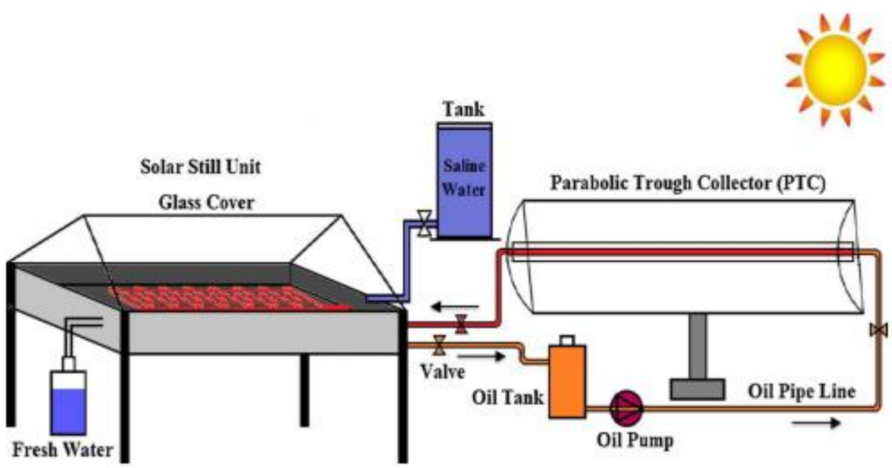

Figure 1. Schematic diagram of the experimental [38].

2 THERMAL CONDUCTIVITY OF CERAMIC MATERIALS USED FOR THERMAL INSULATION

By acting as thermal barrier coatings, these materials promote thermal insulation by preventing the heat from the absorber from escaping and enhancing the performance of the collector[9].As heat barrier coatings ,the following ceramics are used[13] As in the table(1) .

Table 1. Thermal conductivity of ceramic materials used for thermal insulation[14]

Ceramic materials	Thermal conductivity w/m.k
Mullite ($3Al_2O_3.2SiO_2$)	3.5
Titania(TiO_2)	4.8
Magnesium oxide(mgo)	8

2.1 MULLITE ($3AL_2O_3.2SIO_2$)

Due to its advantageous thermal and mechanical characteristics, mullite has attained extraordinary relevance as a material for both conventional and modern ceramics. Mullite exhibits different Al to Si ratios corresponding to the solid solution $Al_{4+2x}Si_{2-2x}O_{10-x}$, where x denotes the number of missing oxygen atoms in the mullite formula .where x varies between approximately 0.2 and 0.9 (corresponding to around 55 to 90 mol% Al_2O_3). A variety of foreign atoms and transition metal cations can be incorporated Depending on the conditions and temperature during synthesis, mullite can form. The crystal structure of mullite is closely similar to that of sillimanite, which is distinguished by parallel-to-the-crystallographic-c-axis chains of edge-connected AlO_6 octahedra. Tetrahedral chains made of $(Al,Si)O_4$ tetrahedra cross-link these extremely rigid chains. Contrary to the comparatively long, compliant Al-O(D) links parallel to b, the tetrahedra are attached to the relatively short, stiffer Al-O(A, B) bonds parallel to a. Some of the mullite's oxygen atoms that connect the tetrahedra are used for charge adjustment. are removedT_3O groups, also known as tetrahedral triclusters, and oxygen vacancies are produced as a result. The anisotropy of mullite's physical characteristics is significantly influenced by the anisotropy of its bonding system [15].

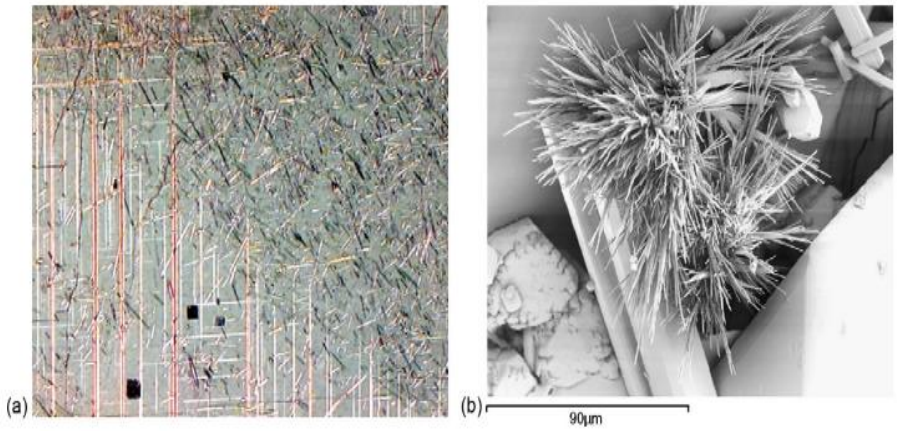

Figure 2. Natural mullite. (a) Mullite was originally described in nature in a thin section micrograph of the lava from Scotland's Island of Mull's volcano Ben More. Keep in mind the presence of microscopic mullite needles that plagioclase has developed over. (b) Hydrothermally created mullite needles in minute druses of volcanic rocks from the Eifel mountain, Germany, as seen under an electron microscope. B. Ternes' courtesy.

2.2 Titanium dioxide

Titanium oxide, often known as titania, can be found in nature. It is a versatile substance with a broad range of uses Some properties of titanium oxide are shown in the table(2). As a photocatalyst, (TiO2) is utilized for its low cost, non-toxicity, and chemical inertness. TiO2 is utilized in many different industrial sectors, including sun screens, paint [16].

Table 2. Properties of titanium dioxide[17] .

Properties	TiO_2-NP
Appearance	White Powder
Crystalline Structure	80% Anatase, 20% Rutile
Primary Particle Size (nm)	21
Average Particle Size (nm)	-
Particle Shape	-
	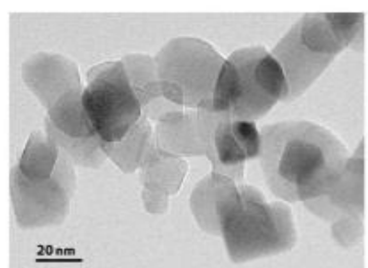
pH	-
Specific gravity (g mL^{-1})	-
Tamped density (g L^{-1})	130
Specific surface area (m^2 g^{-1})	50
Content (wt%)	>99.5

2.3 Magnesium oxide or magnesium

Is an alkaline earth's metal oxide. most of the magnesium oxide that is now manufactured is made by calcining minerals that are found in nature. MgCO3-magnesite is the most typical kind. Seawater, underground brine deposits, as well as deep salt flats where magnesium hydroxide [Mg(OH)2] is found. is treated are other significant sources of magnesium oxide. Magnesium, which makes up around 2% generally 0.12% of saltwater and 0.12% of the earth's crust, is the eighth most plentiful element in the universe.Magnesium is frequently utilized as a refractory brick in the steel industry. For the best It is typically impregnated with carbon (tar, pitch, or graphite) to increase corrosion resistance in environments where basic slags are present, particularly in BOF furnaces or slag lines of treatment ladles [18], As show in figure(3).

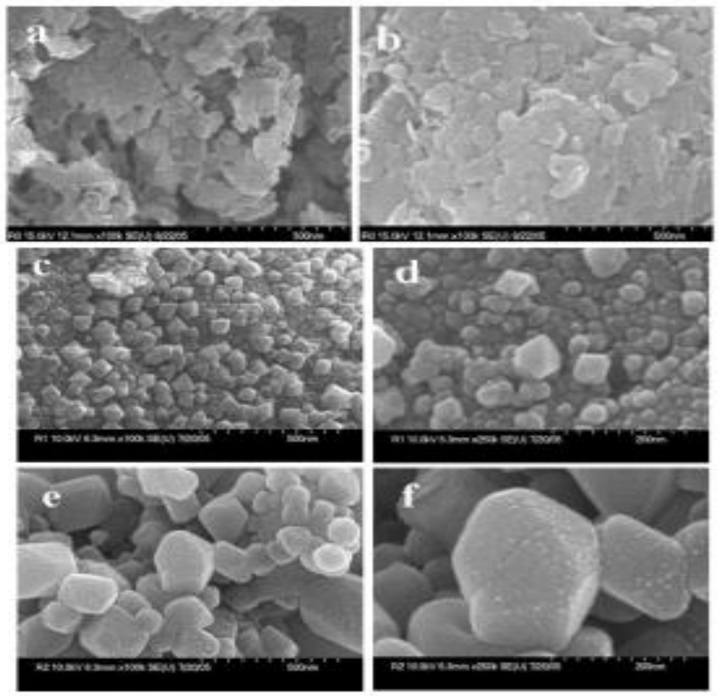

Figure 3. (a) and (b): (c), (d), (e), and (f) show the cubic form of magnesium oxide nanoparticles that have been annealed at 300°C and 500°C for two hours in air[18].

.

3 TYPES OF COATING PROCESS

3.1 Air plasma spray

The deposition of TBCs is frequently accomplished using the air plasma spray (APS) method ,As show in figure(4). In this procedure, Ceramic powder is injected into a plasma jet at high temperature and speed. 7wt% Y2O3 and ZrO2 (7YSZ). The powder is heated and launched in the direction of the substrate. These molten specks harden and produce "splats" upon impact. The building of the ceramic coating is caused by the accumulation of splats. The very poor deposition of the coating, which contains porosity and microcracks, is a factor in the APS TBCs' low heat conductivity. Cracks first show up at the splat interface because it has a lot of porosity, is unstable, and is weak. A solution precursor plasma spray (SPPS) is used to deposit various ceramic coatings. method has recently been devised.3,5–8 It has been proven that the SPPS technique can create 7YSZ TBCs with a high level of durability and low thermal conductivity.3,5 An aqueous chemical precursor feedstock is introduced into the plasma jet during the SPPS process. Before the droplets settle as a 7YSZ coating on the substrate, they go through a series of process, both physical and chemical. The microstructure of the SPPS TBC is distinct, with vertical fissures running throughout a porous matrix and no coarse splats the minuscule amount of unmelted particles and ultra-fine splats produced by the plasma jet's solution precursor make up the matrix of the coating. The TBC gains strain tolerance from the through-thickness cracks, the porosity, and the unmelted granules, while the porosity aids in lowering the heat conductivity [19].

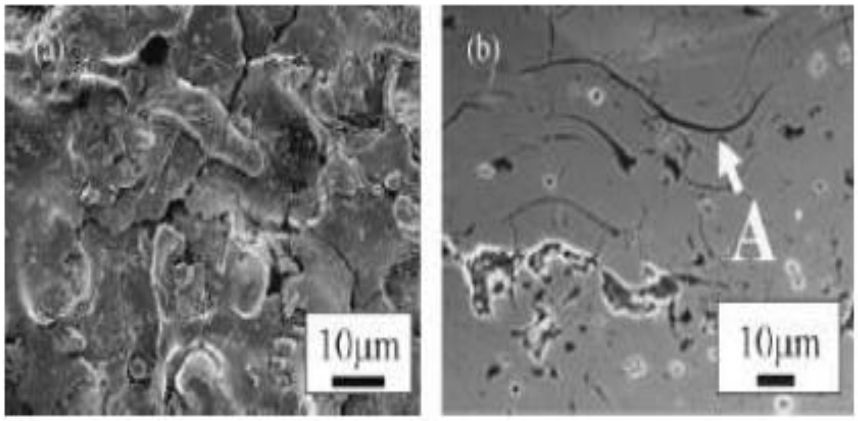

Figure 4. Microstructure of as-sprayed air plasma spray coating: (a) surface morphology; (b) polished cross section [19].

3.2 Physical vapor deposition using an electron beam (EB-PVD)

Some of the issues with the CVD, PVD, and metal spray procedures have been resolved by the electron beam-physical vapor deposition (EB-PVD) approach. electron cannons that focus high-energy electron beams are utilized in the EB-PVD process As show in figure(5), to melt and evaporate ingots and pre-heat the substrate inside the vacuum chamber. Six electron beam guns are employed Four of these are used to evaporate the coating components in Penn State's industrial pilot Sciaky EB-PVD unit, and two are utilized to warm the substrate to promote coating adhesion. The 45 kW of each gun power output. Up to three ingots with dimensions of 450 mm in length and 49–68 mm in diameter can fit in the chamber. The producing unit's overall size is around 1 cubic meter. The substrate can be utilized with a maximum weight of around 100 kg and a maximum diameter of about 400 mm. It can rotate at a speed between 5.5 and 110 rpm. The device additionally includes a three-axis part manipulator and a horizontal sample holder Includes: two 0-14 rpm rotating axes and an 0-4,000 mm/min translation axis. Up to 20 kg of samples can be transported using it. Since EB-PVD is largely a line-of-sight technique, it is possible to achieve uniform coatings on complicated elements (like turbine blades) by rotating the part continuously throughout the coating process [20] .

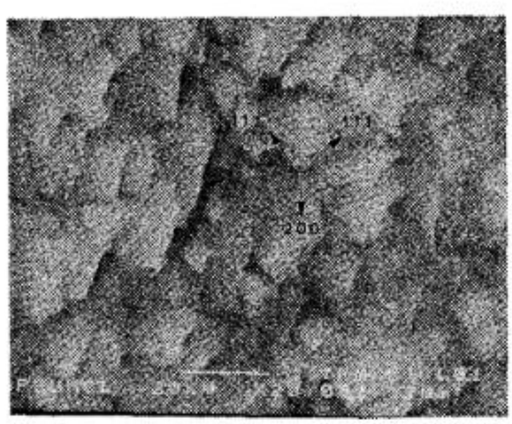

Figure 5. TiN coating's surface morphology as seen in a SEM micrograph. applied by IBAD and EB-PVD to stainless steel substrate[20].

3.3 Spray air brushing

Spray airbrushing is the preferred method for coating materials since it is the simplest, cheapest, and doesn't induce phase changes or oxidation. The covering of the conducting and insulating materials was done using a spray airbrush technique. The most basic form of pneumatic-based technology is sprayed airbrush guns. Surface characteristics of the substrate, including temperature, roughness, and wettability, have a significant impact. The primary purpose of the airbrush pistol is to atomize the liquid (solution) coming out of the nozzle with pressurized air or gas (e.g., nitrogen or argon). As the fluid travels through the nozzle, it breaks up into droplets. The parameters that affect the atomization process include fluid density, viscosity, surface tension, air or gas flow velocity, and nozzle style, As shown in figure(5),[11].

3.3.1 The amount of coating material used, coating velocity, droplet volumes, and surface characteristics can all affect how the layer is formed. The following components make up the setup system:

1. Spray gun: The solution is atomized using the nozzle,
2. a vessel used to hold liquid or a suspension is a container,
3. Air is pumped into the spray cannon using an air compressor. Around 15 centimeters separate the nozzle from the sample surface. Around a 1.5 mm pinhole makes up the nozzle,[12] .

4 SPRAY Air Brush Method and Electron Beam physical Vapor Deposition

4.1 Spray Air Brush Method

manufacturing Spray air brush method The top coating materials deposited by using air brush spray gun is nozzle contain atomization the coating solution coating thickness 300-830 µm [22]. thermal conductivity 0.6-0.99 w / m.k Less durability from EB - PVD, cost Cheap,[12][23].

4.2 (Electron Beam Physical Vapour Deposition) EB – PVD

(Electron Beam Physical Vapour Deposition) EB - PVD Electrons assault the topcoat material , which then evaporates and is deposited on the substrate ,coating thickness Typically 125 am,thermal conductivity 15-2.0 µw / m .k , More durability than spray air brush method , cost Expensive and the applications Turbine blades and vanes in aircraft engines [24].

Table 3. the properties of spray air brush method and (EB-PVD) [25][26]

spray air brush	(EB-PVD)
1-Lower cost	1-Higher cost
2-simple	2-more complex from spray air brush
3-no phase transformation	3 -phase transformation happened
4-coating thickness controlled easy	4- coating thickness controlled

Table 4. Various coating techniques

Technique Name	Description	Ref.
1- Anodizing	Aluminum can be coated with oxidation via the process of anodizing, which uses an electric current to induce a chemical reaction at room temperature. The result is the creation of a layer that can shield the metal from corrosion. This study's goal was to characterize the effects of changes in electric voltage on the surface hardness of the aluminum anodizing series.	[27][28]
2- Galvanizing	In many anticorrosion engineering applications, existing hot-dip galvanized steel (HDG) is repaired using cold galvanizing coatings (CGCs), but the CGC's weak adherence prevents widespread use in the industrial sector.	[29]
3- Electroplating	The most popular technique for coating metals on polymers is electroplating, whose adherence is guaranteed by surface chemical and mechanical interactions. Sadly, there have been discussions about the relative contributions of these elements to total adhesion for the past century without any quantifiable results for the electroplating scenario.	[30]
4- Powder Coating	The basic metal is safeguarded by the coating against mechanical and environmental harm. An essential characteristic of the coating is its resistance to abrasive wear. This paper's goal is to investigate the scratch and wear resistance of epoxy resin powder coatings.	[31][32]

5 PREVIOUS STUDIES

5-1 Seiji Kuroda, Zhensu Zeng a,b, Nobuaki Sakoda, Toshiro Tajiri,(2008). [33] have learned The features of 316L stainless coatings created using an HVAF technique were contrasted with coatings sprayed using an HVOF procedure. The HVAF coatings were typically porous when they were first sprayed. For the coating created with powder of big particles, pores were more noticeable. Through the impingement created by the next sprayed particles, the initially-deposited porous layer by the HVAF system became denser. However, there were still a sizable number of through pores connecting to the substrate that were difficult to see optical microscopy on cross sections with metallographic polish. The HVAF coatings' area proportion of oxides ranged from 3 to 7%. Higher powder feed rates and larger particle sizes resulted in lower oxide content, but the adhesion strength dropped from 34 to 17 MPa. These are significantly lower than the adhesion strength and oxide fraction of the HVOF coating, which are 45–50 MPa and 15–17%, respectively. These results demonstrate that the amount of through holes determines how resistant stainless steel coatings are to corrosion when applied to carbon steel.

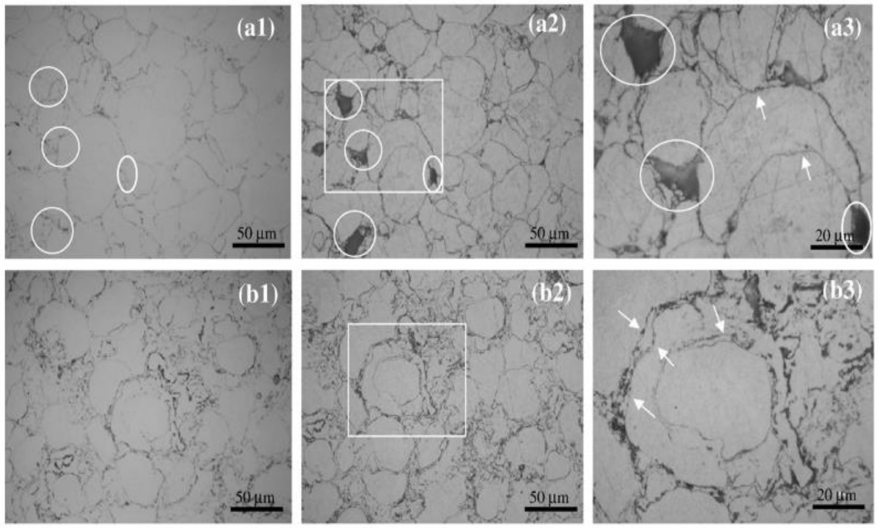

Figure 6 Microstructures of coatings' surfaces after being sprayed with powder B and at 200 g/min (HVAF) and 60 g/min (HVOF) spray rates using a 3 mm spray pitch. (a1) HVAF coating prior to etching, (a2) After etching, HVAF coating, (a3) high-power magnifying (a2), (b1) HVOF coating before etching, (b2) Following HVOF coating and etching, (b3) high-power magnifying (b2).[33]

5-2 Hadi Savaloni, Farzaneh Modiri,(2020) [34] also explored how the type of coating used affects the surface morphology. There is just one time constant involved in the corrosion of manganese nitride coatings, according to the coatings on the sample Mn(293)/SS304L Nyquist curves. Studying the degree of corrosion at various solution temperatures led us to the conclusion that while resistance to corrosion diminishes with temperature, porosity is strongly connected with it. Therefore, based on the results of the analyses, we draw the conclusion that the resistance of the layer is not greatly altered when manganese is deposited on the stainless steel SS304L surface**.** In order to improve the surface and resistance of stainless steel, pure manganese cannot be deemed adequate. However, Given that after annealing in nitrogen flow, the sample's surface corrosion resistance in a 0.4 M H2SO4 solution at room temperature was greatly increased, it may be inferred that an important step in the process must be considered is annealing. Reduced grain boundaries will help to increase surface stability and stop electrolytes from penetrating the surface. since grain boundaries are areas where the sample's surface has pores, holes, and fractures.

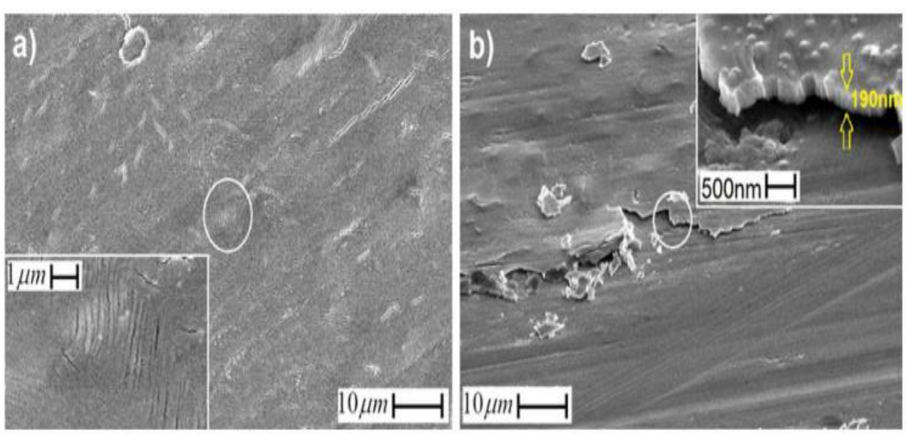

Figure 7. Before annealing, FESEM micrographs of the Mn/SS304L surface and cross section are shown.

5-3 Jelmer Sjollema, Henny C, Devlina Ghosh Colin W. K,(2023).[35] Without regard to their physicochemical characteristics, the objective of this study was to develop a uniform coating mechanism. It also sought to investigate the coating's durability (in vivo) and biocompatibility (in vitro) on different implant surfaces. We speak of this brand-new nGel covering. as a universal coating technique because it was effectively applied to all 11 different medically significant materials. It is a simple process that is quick, affordable, and very reproducible. The AFM images showed that the nGel-coated surfaces were homogeneous. To demonstrate the principle, The coating was FITC-labeled, and the emission of fluorescent signals showed that the primary amines in the nGel's perimeter had successfully bound to the dye's thioisocyanate. When evaluated in vitro (in PBS and FBS solutions, at body temperature, and under dynamic conditions), the nGel-based coatings employed on a variety of substrates showed to be exceptionally stable. Mice were used for the in vivo tests, and the tissue response to coated and uncoated PVDF was comparable, particularly at day 13, as evidenced by similar immune cell infiltration, FBGC production, collagen deposition, and blood vessel creation. Therefore, it can be said that PVDF mesh covered with nGel and based on pNIPMAM is just as biocompatible as pure PVDF. Depending on the desired biomedical use, In the future, the coating may incorporate a variety of features, including antifouling, antibacterial properties, anticancer drugs, or imaging modalities, potentially generating a highly functional and multimodal system. The fundamental benefit of the coating technique is that it is no longer restricted to a single type of material, making translation to a variety of applications viable. Additionally, there is a lot of room for exploration in terms of translation to the clinic.

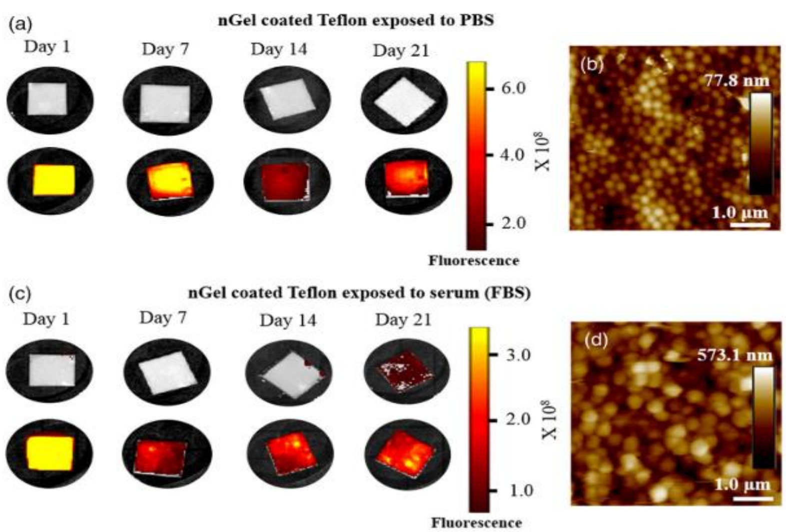

Figure 8. surfaces with p(NIPAM-co-APMA) coatingnGel was put through a stability test.. a) Fluorescence pictures taken by IVIS at 1, 7, 14, and 21 days, expressed in radiant efficiency (p s?1 cm?2 sr?1]/ [Wcm?2) for Teflon coated with nGel and tagged with fluorescein isothiocyanate (FITC) and subjected to potassium phosphate saline (PBS); b) PBS-exposed nGel-coated Teflon captured in an AFM image at day 21; c) same as (a), FITC-labeled Teflon that has been coated with nGel and subjected to fetal bovine serum is the next. (FBS); d) same as (b), The subject at hand is Teflon coated with nGel and subjected to FBS on day 21. (The lowest point of the height bar corresponds to 0 nm.).

5-4 Andrei Zinine, Javier Parrondo, Takashi Hattori,(2023).[36] debated on The results of TiO_2-CeO_2 nanocoating on Spin coating methods on 304LN stainless steel reveal that the coating has photogenerated cathodic protection. protective capabilities. After the corrosion test, the 10% TiO_2-CeO_2 coating exhibits no pinholes or pits. The SEM analysis supported this. Better corrosion resistance outcomes are produced by the contact angle. This coating's resistance to corrosion brought on by NaCl assault was verified. It was discovered that the 10% coatings, as opposed to the 1%, 5%, and 20%

coatings, guaranteed 304LN steel's resistance to corrosion. The quantity of fractures and defects generated by spin coating methods may rise with increased concentration. The TiO_2-CeO_2 coating can provide greater photogenerated cathodic protection to a metal substrate when lighting is available in addition to acting as a superior anticorrosive barrier when lighting is absent. Regardless of whether there is lighting, this is true. With the use of a solution containing 3.5 percent NaCl, the coating's wettability and corrosion resistance were assessed. The weight percentage of the coating helps to increase the material's corrosion resistance. The corrosion started to slow down after 600 hours submerged in a solution of 3.5% NaCl. The deposits were examined using energy dispersive spectroscopy (EDS), X-ray diffraction (XRD), and scanning electron microscopy (SEM). The nano composites' physical properties enable them to stick to surfaces. The ratio of surface to volume is good. The concentration of the water will increase as the contact angle decreases.

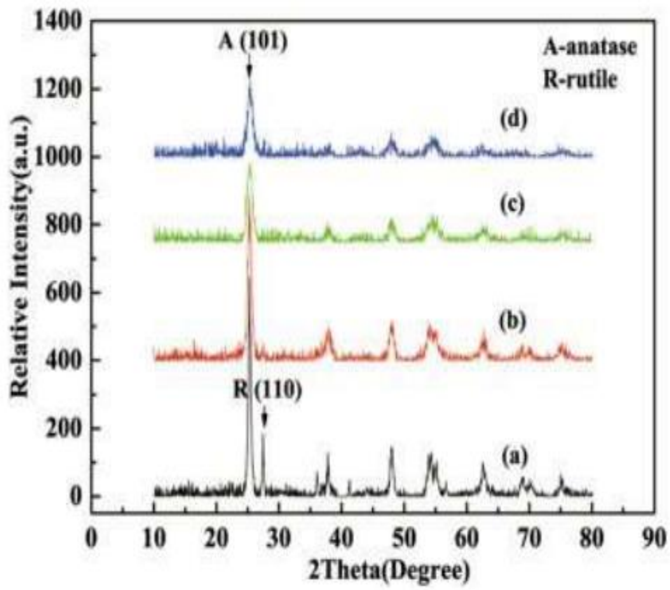

Figure 9. Coatings made of TiO_2-CeO_2 XRD pattern.

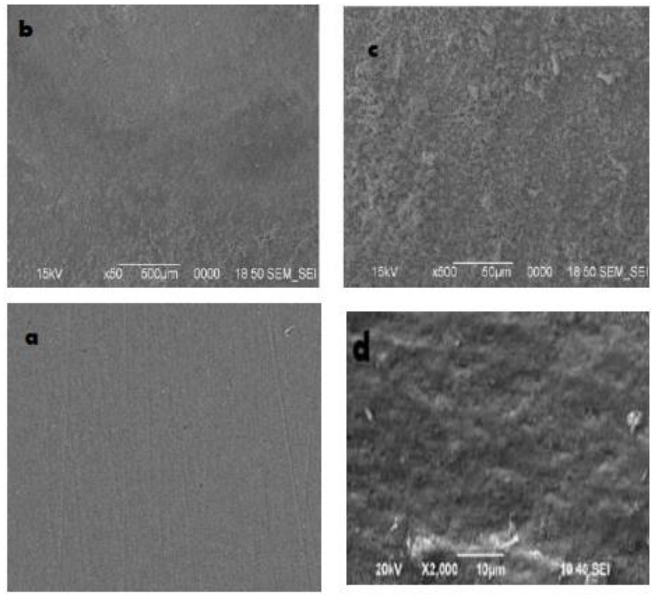

Figure 10. SEM pictures of (a) 304LN as received
(b) 1% TiO2-CeO2coating (c) 10% TiO2- CeO2coatingand (d) 20% TiO2-CeO2coating
.

5-5 Zhaolin Tang, Pooria Najafisayar , Maryam Yaghtin 2,(2023).[37] The relationships between YSZ suspension parameters, processing parameters, the suspension atomization behavior and the resulting SPS coatings' microstructures were investigated. YSZEt suspensions atomized droplets are smaller (12.4 μm) than the droplets of YSZH- Et and YSZH (18.7 and 21.7μm, respectively). This leads to deposition of coatings with columnar microstructures from ethanol-based suspension (YSZEt) coatings.Both the water based (YSZH) and mixed water-ethanol (YSZHEt) suspensions coatings exhibited lamellar microstructures. Coatings with more pronounced columnar structures were obtained from deposition on substrates with higher surface roughness, at longer spray distances. Water-based suspensions including α-Terpineol dispersant (YSZH- αT-2.5) exhibited favorable rheological properties to produce smaller droplet sizes in atomized phase. Ethanol can be replaced with water if appropriate dispersant (like α-Terpineol) and pH value is selected, in order to produce SPS coatings with columnar morphology, without altering other processing parameters (like substrate surface roughness and spray distance).

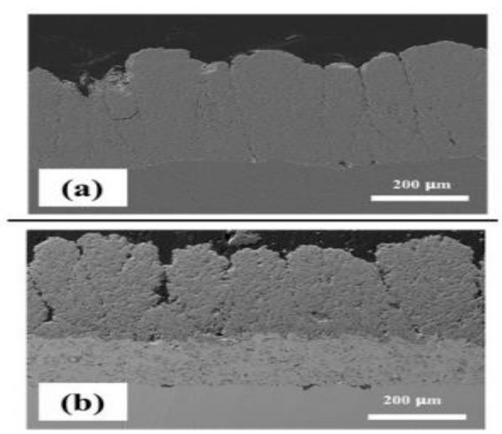

Figure 11. Cross sectional SEM micrographs and their relevant surface profiles attributed to the coatings that were deposited from (a) YSZEt and (b) YSZH- αT- 2.5 suspensions.

6 CONCLUSION

A Making use of solar energy, one of the least expensive renewable energy sources, to reduce reliance on fossil fuels, which are expensive and complex to manufacture.

- Lowering the cost of manufacturing a solar collector by employing readily accessible and affordable ceramic materials and easy coating techniques to create a solar collector with high heating efficiency.
- Ensuring that home water heating is continuous and preventing electrical power issues and outages. Additionally, minimizing the usage of electric energy generated by fossil fuel-powered power plants reduces the pollution and hazardous emissions brought on by the burning of fuels.
- Using selected ceramic as thermal insulation increases the efficiency of solar thermal collectors.

REFERENCES

1. T. Alam *et al.*, "Performance augmentation of the flat plate solar thermal collector: A review," *Energies*, vol. 14, no. 19, pp. 1–23, 2021, doi: 10.3390/en14196203.

2. M. M. Peiravi and J. Alinejad, "Hybrid conduction, convection and radiation heat transfer simulation in a channel with rectangular cylinder," *J. Therm. Anal. Calorim.*, vol. 140, no. 6, pp. 2733–2747, 2020, doi: 10.1007/s10973-019-09010-0.

3. D. S. R. Krishna and Y. Sun, "Thermally oxidised rutile-TiO 2 coating on stainless steel for tribological properties and corrosion resistance enhancement," *Appl. Surf. Sci.*, vol. 252, no. 4, pp. 1107–1116, 2005, doi: 10.1016/j.apsusc.2005.02.046.

4. J. W. Oldfield and B. Todd, "Technical and economic aspects of stainless steels in MSF desalination plants," *Desalination*, vol. 124, no. 1–3, pp. 75–84, 1999, doi: 10.1016/S0011-9164(99)00090-9.

5. M. Fini *et al.*, "A new austenitic stainless steel with negligible nickel content: An in vitro and in vivo comparative investigation," *Biomaterials*, vol. 24, no. 27, pp. 4929–4939, 2003, doi: 10.1016/S0142-9612(03)00416-2.

6. Y. Sun and T. Bell, "Sliding wear characteristics of low temperature plasma nitrided 316 austenitic stainless steel," *Wear*, vol. 218, no. 1, pp. 34–42, 1998, doi: 10.1016/S0043-1648(98)00199-9.

7. N. Tabet, I. Allam, and R. C. Yin, "X-ray photoelectron spectroscopy investigation of the carburization of 310 stainless steel," *Appl. Surf. Sci.*, vol. 220, no. 1–4, pp. 259–272, 2003, doi: 10.1016/S0169-4332(03)00820-1.

8. L. Gong, Y. Wang, X. Cheng, R. Zhang, and H. Zhang, "Porous mullite ceramics with low thermal conductivity prepared by foaming and starch consolidation," *J. Porous Mater.*, vol. 21, no. 1, pp. 15–21, 2014, doi: 10.1007/s10934-013-9741-z.

9. X. Q. Cao, R. Vassen, and D. Stoever, "Ceramic materials for thermal barrier coatings," *J. Eur. Ceram. Soc.*, vol. 24, no. 1, pp. 1–10, 2004, doi: 10.1016/S0955-2219(03)00129-8.

10. S. Kuroda, J. Kawakita, M. Watanabe, and H. Katanoda, “Warm spraying - A novel coating process based on high-velocity impact of solid particles,” *Sci. Technol. Adv. Mater.*, vol. 9, no. 3, 2008, doi: 10.1088/1468-6996/9/3/033002.

11. B. Fotovvati, N. Namdari, and A. Dehghanghadikolaei, “On coating techniques for surface protection: A review,” *J. Manuf. Mater. Process.*, vol. 3, no. 1, 2019, doi: 10.3390/jmmp3010028.

12. J. Li, J. Liang, and Y. Liu, “High-thermal conductive coating used on metal heat exchanger,” *Chinese J. Chem. Eng.*, vol. 22, no. 5, pp. 596–601, 2014, doi: 10.1016/S1004-9541(14)60068-9.

13. J. Long, C. Jiang, J. Zhu, Q. Song, and J. Hu, “Controlled TiO2 coating on hollow glass microspheres and their reflective thermal insulation properties,” *Particuology*, vol. 49, pp. 33–39, 2020, doi: 10.1016/j.partic.2019.03.002.

14. J. Xiao, W. Chen, L. Wei, W. He, and H. Guo, “Mechanical properties and thermal conductivity of ytterbium-silicate-mullite composites,” *Materials (Basel).*, vol. 13, no. 3, 2020, doi: 10.3390/ma13030671.

15. H. Schneider, J. Schreuer, and B. Hildmann, “Structure and properties of mullite — A review,” vol. 28, pp. 329–344, 2008, doi: 10.1016/j.jeurceramsoc.2007.03.017.

16. S. I. Kunya, J. S. Polytechnic, and A. Yunusa, “PROPOSAL FOR HYDROTHERMAL TECHNIQUE FOR METAL OXIDE NANOMATERIAL SYNTHESIS : THE CASE OF ZnO AND TiO2,” no. October, 2022.

17. K. Samree *et al.*, “Enhancing the antibacterial properties of PVDF membrane by hydrophilic surface modification using titanium dioxide and silver nanoparticles,” *Membranes (Basel).*, vol. 10, no. 10, pp. 1–18, 2020, doi: 10.3390/membranes10100289.

18. G. Bassioni, R. Farid, M. Mohamed, R. M. Hammouda, and F. E. Kühn, *Effect of different parameters on caustic magnesia hydration and magnesium hydroxide rheology: A review*, vol. 2, no. 20. 2021. doi: 10.1039/d0ma00887g.

19. D. Chen, M. Gell, E. H. Jordan, E. Cao, and X. Ma, “Thermal stability of air plasma spray and solution precursor plasma spray thermal barrier coatings,” *J. Am. Ceram. Soc.*, vol. 90, no. 10, pp. 3160–3166, 2007, doi: 10.1111/j.1551-2916.2007.01864.x.

20. Singh, J., Quli, F., Wolfe, D. E., Schriempf, J. T., & Singh, J. (1999). An overview: Electron beam-physical vapor deposition technology-Present and future applications. Applied Research Laboratory, Pennsylvania State University, USA.

21. T. Arunkumar, K. Vinothkumar, A. Ahsan, R. Jayaprakash, and S. Kumar, “Experimental Study on Various Solar Still Designs,” *ISRN Renew. Energy*, vol. 2012, pp. 1–10, 2012, doi: 10.5402/2012/569381.

22. A. J. Slifka, B. J. Filla, and J. M. Phelps, “Thermal Conductivity of Magnesium Oxide from Absolute, Steady-State Measurements,” *J. Res. Natl. Inst. Stand. Technol.*, vol. 103, no. 4, pp. 357–363, 1998, doi: 10.6028/jres.103.021.

23. K. Ravikumar, C. N. Raju, and M. Saheb, “CFD Analysis of a Cross-flow Heat Exchanger with Different fin thickness,” vol. 13, no. 2, pp. 345–362, 2017.

24. M. Romero, I. Padilla, M. Contreras, and A. López-delgado, “Mullite-based ceramics from mining waste: A review,” *Minerals*, vol. 11, no. 3, pp. 1–39, 2021, doi: 10.3390/min11030332.

25. N. F. Asri, T. Husaini, A. B. Sulong, E. H. Majlan, and W. R. W. Daud, “Coating of stainless steel and titanium bipolar plates for anticorrosion in PEMFC: A review,” *Int. J. Hydrogen Energy*, vol. 42, no. 14, pp. 9135–9148, 2017, doi: 10.1016/j.ijhydene.2016.06.241.

26. M. Meikandan, P. Ganesh Kumar, D. Sakthivadivel, V. S. Vigneswaran, and K. Malar Mohan, “Multi-wall carbon nanotubes coating on a copper substrate using airbrush spray coating,” *Proc. Inst. Mech. Eng. Part E J. Process Mech. Eng.*, vol. 235, no. 2, pp. 285–291, 2021, doi: 10.1177/0954408920959157.

27. A. S. Darmawan, T. W. B. Riyadi, A. Hamid, B. W. Febriantoko, and B. S. Putra, “Corrosion resistance improvement of aluminum under anodizing process,” *AIP Conf. Proc.*, vol. 1977, 2018, doi: 10.1063/1.5042862.

28. A. Gasco-Owens, D. Veys-Renaux, V. Cartigny, and E. Rocca, “Large-pores anodizing of 5657 aluminum alloy in phosphoric acid: an in-situ electrochemical study,” *Electrochim. Acta*, vol. 382, 2021, doi: 10.1016/j.electacta.2021.138303.

29. J. Li *et al.*, “Interface characteristics and anticorrosion performances of cold galvanizing coatings incorporated with -chloropropyl triethoxysilane on hot-dip galvanized steel,” *Coatings*, vol. 11, no. 4, 2021, doi: 10.3390/coatings11040402.

30. R. Melentiev, R. Tao, and G. Lubineau, “Towards decoupling chemical and mechanical adhesion at the electroplated metal / polymer interface via precision surface texturing,” no. April, 2023, doi: 10.1016/j.surfin.2023.102875.

31. A. K. Chatre, “Analysis of Wear and Strength Behaviour of SiO2 Nanoparticles Mixed in Epoxy Powder Coating on Mild Steel Material,” *Int. J. Res. Appl. Sci. Eng. Technol.*, vol. 8, no. 12, pp. 130–135, 2020, doi: 10.22214/ijraset.2020.32430.

32. C. Harliman and K. Pasaribu, “Analisa Produktivitas Single dan Multifaktor Mesin Manual dan Otomatis pada Perusahaan Powder Coating PT TKM di Bekasi Christie Harliman Kurniawan Pasaribu,” 2021.

33. Z. Zeng, N. Sakoda, T. Tajiri, and S. Kuroda, “Structure and corrosion behavior of 316L stainless steel coatings formed by HVAF spraying with and without sealing,” *Surf. Coatings Technol.*, vol. 203, no. 3–4, pp. 284–290, 2008, doi: 10.1016/j.surfcoat.2008.09.011.

34. F. Modiri and H. Savaloni, “A study of the corrosion of stainless steel 304L coated with a 190 nm-thick manganese layer and annealed with nitrogen flux in a 0.4-mole solution of H2SO4 at different temperatures,” *J. Theor. Appl. Phys.*, vol. 14, no. 1, pp. 21–35, 2020, doi: 10.1007/s40094-019-00345-5.

35. P. van R. D. Keskin, D. Ghosh, C. Rosman, R. Bron, A. M. Forson, C. Siebenmorgen, G. Zu, T. van Kooten, J. Sjollema, H. van der Mei, M. Witjes, “A universal nanogel-based coating approach for medical implant materials,” *Adv. Healthc. Mater.*, vol. Submitted, pp. 1–14, 2021, doi: 10.1002/anbr.202200141.

36. M. Kripa Suvarna, “A Study on TiO2-CeO2nanocomposite coatings for corrosion protection of 304LN stainless steel,” *J. Phys. Conf. Ser.*, vol. 2484, no. 1, 2023, doi: 10.1088/1742-6596/2484/1/012021.

37. A. Yaghtin, M. Yaghtin, P. Najafisayar, and Z. Tang, “On the Applicability of Modified Water based YSZ Suspensions to Produce Plasma Sprayed Columnar Coatings,” no. June, pp. 1–11, 2023, doi: 10.20944/preprints202306.0566.v1.

38. M. Fathy, H. Hassan, and M. Salem Ahmed, “Experimental study on the effect of coupling parabolic trough collector with double slope solar still on its performance,” *Sol. Energy*, vol. 163, no. August 2017, pp. 54–61, 2018, doi: 10.1016/j.solener.2018.01.043.